JOURNAL OF COMPUTATIONAL PHYSICS 86, 466–486 (1990)

An Iterative Method to Solve the Nonlinear Poisson's Equation in the Case of Plasma Tangential Discontinuities

M. ROTH AND J. LEMAIRE

Institute for Space Aeronomy, 3 avenue Circulaire, B-1180 Brussels, Belgium

AND

A. MISSON

Centre de Recherches en Physique des Plasmas - Ecole Polytechnique de Lausanne, 21, avenue des Bains, 1007 Lausanne, Switzerland

Received March 22, 1988; revised April 13, 1989

In order to determine the electric potential in collisionless tangential discontinuities of a magnetized plasma, it is required to solve a non-linear Poisson's equation with sources of charge and current depending on the actual potential solution. This non-linear second-order differential equation is solved by an iterative method. This leads to an ordered sequence of non-linear algebraic equations for each successive approximation of the actual electric potential. It is shown that the method holds for transitions with characteristic thicknesses (D) as thin as five Debye lengths (λ). For smaller thicknesses, when D shrinks to 3λ or less, the method fails because in that case the iteration procedure does no longer converge. Numerical results are shown for an ion-dominated layer ($D \sim 10^2 - 10^3\lambda$), as well as for two electron-dominated layers characterized by $D \approx 5\lambda$ and $D \approx 2.5\lambda$, respectively. In all cases considered in this paper, the relative error on the electric potential obtained as a solution of the quasi-neutrality approximation is of the order of the relative charge density. When the method holds, each successive approximation reduces the relative error on the potential by roughly a factor of 10. For space plasma boundary layers, the quasi-neutrality approximation can be used with much confidence since their thickness is always much larger than the local Debye length.

1. INTRODUCTION

It is generally considered that in astrophysical and geophysical plasmas the electron density balances almost exactly the ion charge density; i.e., plasmas are quasi-neutral. Nobody questions that this is a very satisfactory approximation in uniform or nearly uniform plasma regions of space.

However, it has sometimes be questioned whether this approximation is still a

0021-9991/90 $3.00

valid one at the earth's magnetopause [1] or at other sharp boundary layers where the physical properties of the plasma (density, temperature, bulk speed, magnetic field, ...) change abruptly from one set of values to another one. The magnetospheric bow shock [2] is another type of boundary where a significantly large electric charge separation might be expected.

The purpose of this work is to verify on a few case studies that the quasi-neutrality equation is indeed a valid zero-order approximation when the boundary layer has a thickness much larger than the characteristic Debye length.

One of the simplest type of boundary layer or plasma discontinuity observed in space is the so-called planar "tangential discontinuity" (TD for short). In the reference frame tied to a TD there is no plasma crossing the layer. In addition, the magnetic field component along the normal to the boundary vanishes. Furthermore, from conservation laws [3], the total plasma and field pressure across a TD does not vary. However, the plasma velocity distribution and the tangential magnetic field (intensity and direction) are both varying over short distances, as at the interface of ferromagnetic domains in solid-state plasmas. TDs have been found to be abundant in the solar wind [4] and observations indicate that the earth's magnetopause can sometimes be considered as a tangential discontinuity [5].

To make theoretical models of steady-state collisionless TDs, the plasma kinetic method has been used by a number of authors [6–13]. Actually, the Maxwell's equations for the electric and magnetic fields are combined with the Vlasov equation for the particles. The result is a set of second-order non-linear differential equations for the electric and magnetic vector potentials, with sources of charge and current depending on the actual potentials.

The solution of the Vlasov equation is based on the standard methods of constructing distribution functions in terms of the conserved energy and generalized momenta of the particles. It is then a relatively straightforward task to produce solutions which mimic a number of observed steady-state boundary layers [6]. This method is preferable to particle simulation involving a time dependent problem which leads to the set-up of steady-state electric and magnetic structures. Indeed, for typical space plasmas where the number of particles in a Debye sphere is of the order of 10^9, particle simulation involves a large number of particles whose trajectories can be determined with efficiency by only high speed, large scale computers. Although particle simulation is particularly useful whenever a limited number of analytic methods are available, this is not the case for the problem under consideration in this paper for which solutions of the Vlasov equation are straightforward.

Numerical difficulties arise, however, when attempts are made to integrate Poisson's equation for the electric potential—a second-order non-linear differential equation—by standard methods (e.g., Runge–Kutta or Hamin). These difficulties arise because the right-hand side of Poisson's equation is a difference between two very large numbers, the electron and ion densities, which are almost exactly equal to each other. A zero-order approximation of the actual electric potential (ϕ) can however be determined as a solution of the quasi-neutrality equation, where the electron density is a very sensitive function of ϕ.

Of course, this zero-order approximation holds whenever the total charge density which is proportional to the Laplacian of ϕ is found a posteriori to be much smaller than the charge density associated with the positively (or negatively) charged particles. Each time this condition is fulfilled, a self-consistent potential is obtained. The aim of this paper is to study the small deviations from quasi-neutrality in TDs. In this case, Poisson's equation for the electric potential must be solved instead of the quasi-neutrality equation. The higher order approximations obtained this way are then compared to the zero-order approximation corresponding to the solution of the quasi-neutrality equation.

In this paper, Poisson's equation has been solved by an iterative method. The procedure leads to successive approximations of the potential starting with the zero-order approximation ϕ_0 which is the solution of the algebraic quasi-neutrality equation. The potential in the approximation of order n ($n>0$) is the solution ϕ_n of a new algebraic equation obtained by replacing the right-hand side of the quasi-neutrality equation by "a charge density," i.e., a quantity proportional to the Laplacian of ϕ_{n-1}. It has been found that, after only a few iterations, the successive approximations do not differ by more than the precision of the computer (nine significant digits), at least for broad layers (the so-called ion-dominated layers in [7]) whose characteristic thickness is the ion gyroradius. For these ion-dominated layers the zero-order approximation ϕ_0 does not differ significantly from higher-order approximations (i.e., $|\phi_n - \phi_0|/|\phi_n| < 3 \times 10^{-6}$) and in practice ϕ_0 can be considered as very close to the actual potential. For thinner layers with thicknesses of the order of an electron gyroradius (the so-called electron-dominated layers in [7]), it is shown that the iterative process is convergent as long as the characteristic thickness (D) does not become smaller than five Debye lengths (λ). The iterative procedure fails however when D shrinks to about 3λ or less. In all cases we have considered so far, the relative error on ϕ_0 (with respect to the actual potential) has been found of the order of the relative charge density.

The model used for a collisionless TD will be briefly described in Section 2. Although equilibrium configurations of TDs in collisionless plasmas under a wide variety of boundary conditions and assumptions have been discussed in the literature (see Ref. [6–13]), the model considered in this paper is a simplified version based on the work of Sestero [7]. Section 3 outlines the iteration process used to solve Poisson's equation. In Sections 4 and 5 are displayed the numerical results obtained for layers with various thicknesses, i.e., an ion-dominated layer (Section 4) and two electron-dominated layers with $D \approx 5\lambda$ and $D \approx 2.5\lambda$ (Section 5). Conclusions are summarized in Section 6.

2. A Kinetic Model of Tangential Discontinuities

For the sake of simplicity, we study steady-state, unidimensional planar current layers which are parallel to the $(y-z)$ plane of a cartesian coordinate system. All plasma and field variables are assumed to depend only on the x-coordinate, normal

to the layer. The magnetic field **B** is oriented along the z-axis while the electric field **E** is parallel to the x-axis. In this model, the z-coordinate is an ignorable coordinate for the motion of a single plasma particle. Therefore, the so-called constants of motion are the energy (H) and the y-component of the generalized momentum (p):

$$H = \tfrac{1}{2} m(v_x^2 + v_y^2) + Ze\,\phi(x) \tag{1}$$

where Ze is the charge ($e = 1.6 \times 10^{-19} C$) of the particle of mass m and v its velocity, while $\phi(x)$ is the electric potential;

$$p = mv_y + Ze\,a(x), \tag{2}$$

where $a(x)$ is the magnetic vector potential (parallel to the y-axis).

Any function of H and p, $F(H, p)$, is a solution of the steady-state Vlasov equation. Consider the following distribution function [7] for a given plasma species:

$$F(H, p) = \delta(p)\,\eta(H) \tag{3}$$

with

$$\begin{aligned} \delta(p) &= C_\ell \qquad \text{if} \quad p \text{ in }]-(\operatorname{sign} Z)\infty, 0] \\ &= C_r \qquad \text{if} \quad p \text{ in } [0, +(\operatorname{sign} Z)\infty[\\ &\quad (\operatorname{sign} Z = +1, \text{ if } Z > 0 \\ &\qquad = -1, \text{ if } Z < 0), \end{aligned}$$

where C_ℓ, C_r are arbitrary ($\geqslant 0$) constants and $\eta(H)$ a Maxwellian distribution given by

$$\eta(H) = \alpha \left(\frac{m}{2\pi kT}\right) \exp\left(-\frac{H}{kT}\right), \tag{4}$$

where T is the asymptotic temperature of the particle species and α is a parameter which has the dimension of a number density.

The distribution function (3) as a product of an exponential in H (the Maxwellian η gives by Eq. (4)) by a step function in p gives conceivably the simplest model describing a sharp transition layer. Note that other choices are possible since for any single-valued distribution function in the whole (H, p) plane the Vlasov equation a priori admits a solution. Thus the state of the plasma at both ends of a TD does not uniquely determine the transition profile. This is a peculiar feature of the nonlinear Vlasov equation [13]. To remove the nonuniqueness of the distribution functions, consideration of particle accessibility in phase space must be met [14]. This requires the knowledge of the characteristics of the plasma in the boundary source regions together with the transport mechanisms bringing the plasma to the transition itself. This problem being outside the scope of this paper we will be content with Sestero's distribution functions (3). Indeed, to illustrate the departure from charge neutrality in thin boundary layers the choice of the distribu-

tion functions is not crucial. Furthermore, the method for solving Poisson's equation developed in the next section would remain conceptually the same for any other choice than the distribution given by (3) and (4).

From (3) and (4), the number density (n) and the current density (j)—parallel to the y-axis—can be computed as a function of ϕ and a. It is found that

$$n = \frac{\alpha}{2} \exp\left(-\frac{Ze\phi}{kT}\right)\left[C_\ell \operatorname{erfc}\left(\frac{a}{2^{1/2} R_a B_a}\right) + C_s \operatorname{erfc}\left(-\frac{a}{2^{1/2} R_a B_a}\right)\right] \tag{5}$$

$$j = \frac{1}{2} |Z| e\alpha (C_s - C_\ell) \left(\frac{2kT}{\pi m}\right)^{1/2} \exp\left(-\frac{Ze\phi}{kT}\right) \exp\left(-\frac{a^2}{2R_a^2 B_a^2}\right), \tag{6}$$

where erfc is the complementary error function

$$\operatorname{erfc}(u) = \frac{2}{\sqrt{\pi}} \int_u^{+\infty} e^{-x^2}\, dx$$

and $R_a B_a$ is a constant given by

$$R_a B_a = \left(\frac{mkT}{Z^2 e^2}\right)^{1/2} \tag{7}$$

with R_a and B_a being some characteristic asymptotic Larmor radius and magnetic field, respectively; i.e.,

$$R_a B_a = R_\ell B_\ell = R_s B_s. \tag{8}$$

In (8), R_ℓ and R_s are the characteristic Larmor radii at $x = -\infty$ (on the left-hand side) and $x = +\infty$ (on the right-hand side), respectively; while B_ℓ and B_s are the magnetic field intensities at $x = -\infty$ and $x = +\infty$, respectively.

The Maxwell equations to solve are

$$\frac{d^2\phi}{dx^2} = -\frac{e}{\varepsilon_0} \sum_{v=1}^{s} Z^{(v)} n^{(v)} \tag{9}$$

$$\frac{d^2 a}{dx^2} = -\mu_0 \sum_{v=1}^{s} j^{(v)}, \tag{10}$$

where ε_0 and μ_0 are the vacuum permittivity and permeability, respectively ($\varepsilon_0 = 8.854 \times 10^{-12}$ F/m, $\mu_0 = 4\pi \times 10^{-7}$ H/m), and s is the number of particle species.

The electric field $(E, 0, 0)$ and the magnetic field $(0, 0, B)$ are the derivatives of potentials, i.e.,

$$E = -\frac{d\phi}{dx} \tag{11}$$

$$B = \frac{da}{dx}. \tag{12}$$

The magnetic and electric field distributions within the boundary layer are then determined by solving the system of differential equations (9) to (12) with $n^{(v)}$ and $j^{(v)}$ given by (5) and (6), respectively. Equations (10) and (12) will be solved using a Hamin's predictor-corrector scheme while (9) and (11) will be solved by using the iteration process described in the next section. The right-hand sides of Eq. (9) and (10) are non-linear functions of ϕ and a. Furthermore, the right-hand side of (9) is a sum of terms which must remain much smaller than each individual term as a consequence of the tendency of plasmas to maintain electric neutrality. For these reasons standard numerical procedures to solve Poisson's equation generally fail to converge.

Note that, in this model, if the electron (/ion) velocity distribution remains Maxwellian from $x = -\infty$ to $x = +\infty$, only the ions (/electrons) can be accelerated inside the transition, on a characteristic scale lengths of the order of a few ion (/electron) Larmor gyroradii. Following Sestero [7], these transitions are called ion- (/electron)-dominated layers, respectively.

3. An Iteration Process to Solve Poisson's Equation

Plasmas being quasi-neutral, $d^2\phi/dx^2 \simeq 0$. Therefore, the zero-order approximation of Poisson's equation (9) is the quasi-neutrality equation:

$$\sum_{v=1}^{s} Z^{(v)} n^{(v)}(a_0, \phi_0) = 0. \tag{13}$$

By introducing the quantity N_{rst} (with the summation extended over all species) defined by

$$N_{rst} = \sum Z K_1^r K_2^s K_3^t n \tag{14}$$

with

$$K_1 = -\frac{Ze}{kT} \tag{15}$$

$$K_2 = \frac{1}{kT} = \frac{1}{|Z| eR_a B_a} \left(\frac{m}{kT}\right)^{1/2} \tag{16}$$

$$K_3 = -\frac{1}{R_a^2 B_a^2}, \tag{17}$$

Eq. (13) can also be written as

$$N_{000}(a_0, \phi_0) = 0. \tag{18}$$

Coupled with the differential equations (10) and (12), (18) can be solved numerically. The potential ϕ_0—and also the higher order approximations $\phi_1, \phi_2, \ldots$ (see below)—is then obtained by the Brent's method of finding the root of a non-linear equation (this method combines root bracketing, bisection and inverse quadratic interpolation [15]).

We also introduce the quantities

$$J_{rst} = \sum Z K_1^r K_2^s K_3^t j \tag{19}$$

and

$$j_{rst} = \sum K_1^r K_2^s K_3^t j. \tag{20}$$

By differentiating (18) twice with respect to x, it is possible to obtain algebraic expressions for the first and second derivatives of ϕ_0. It is found that

$$\phi_0' = -B_0 J_{010}/N_{100} \tag{21}$$

$$\phi_0'' = N_{100}^{-1} J_{010}(\mu_0 j_{000} + 2B_0^2 N_{100}^{-1} J_{110} - B_0^2 N_{100}^{-2} J_{010} N_{200}) - a_0 B_0^2 J_{011} N_{100}^{-1} = \phi_0''(a_0, \phi_0, B_0). \tag{22}$$

To carry out those derivatives, we have used the following differentiation rules:

$$\frac{\partial N_{rst}}{\partial \phi} = N_{r+1,s,t} \tag{23}$$

$$\frac{\partial N_{rst}}{\partial a} = J_{r,s+1,t} \tag{24}$$

$$\frac{\partial J_{rst}}{\partial \phi} = J_{r+1,s,t} \tag{25}$$

$$\frac{\partial J_{rst}}{\partial a} = a J_{r,s,t+1} \tag{26}$$

and for any quantity depending on ϕ, a, and B

$$\frac{d}{dx} = \phi' \frac{\partial}{\partial \phi} + B \frac{\partial}{\partial a} - \mu_0 j_{000} \frac{\partial}{\partial B}. \tag{27}$$

The next approximation for ϕ, i.e., the first-order approximation ϕ_1 is solution of the algebraic equation

$$\sum Zn(a_1, \phi_1) = -\frac{\varepsilon_0}{e} \phi_0''(a_1, \phi_1, B_1) \tag{28}$$

The right-hand side of this equation is given by (22). Equation (28) is coupled with the differential equations (10) and (12) to obtain a_1, ϕ_1, and B_1.

Higher order approximations for ϕ are solutions of algebraic equations of the form:

$$\sum Zn(a_i, \phi_i) = -\frac{\varepsilon_0}{e}\phi''_{i-1}(a_i, \phi_i, B_i). \tag{29}$$

Although the right-hand side of (29) can in principle be obtained by differentiating twice the previous equation for ϕ_{i-1}, the number of terms in the expression for ϕ''_i becomes rapidly large for $i \geqslant 2$. Yet expressions for ϕ'_1 and ϕ''_1 have been obtained and can be found in the Appendix. Fortunately, the determination of expressions for higher order second derivatives is unnecessary because numerical solutions for the second-order approximation show that, even in thin electron-dominated layers, a_2 and B_2 do not differ significantly from a_1 and B_1. Therefore, for orders larger than 2 [$i \geqslant 3$ in (29)], (10) and (12) have been decoupled from (29) and the method used to determine $\phi_2, \phi_3, \ldots$ can be stated as follows:

(1) Coupled with the differential equations (10) and (12), the equation

$$\sum Zn(a_2, \phi_2) = -\frac{\varepsilon_0}{e}\phi''_1(a_2, \phi_2, B_2) \tag{30}$$

controls the second-order approximation for ϕ_2. In this equation, $\phi''_1(a_2, \phi_2, B_2)$ has been obtained by differentiating (28) twice with respect to x. Its mathematical formulation can be found in the Appendix. The coupled equations (10), (12), and (30) are then solved numerically. Their solutions are a_2, ϕ_2, and B_2.

(2) From the set of values for $\phi_2(x)$, the derivatives ϕ'_2 and ϕ''_2 are determined numerically by a Lagrangian method of interpolating polynomials using 5 or 7 points.

(3) From (29), third and higher order approximations for ϕ are successively determined numerically by the Brent's method while keeping the second-order approximation (a_2, B_2) for a and B. From these higher order approximations $(i \geqslant 3)$, ϕ''_3, ϕ''_4..., are also determined numerically by a Lagrangian method of interpolating polynomial.

This iterative method of solving Poisson's equation remains near to the physics sustaining the natural tendency of plasmas to maintain quasi-neutrality. Indeed, each iteration leads to a new potential resulting from the weak charge separation computed in the previous iteration. In a few iterations, the deviation from quasi-neutrality can therefore be easily deduced. When the iterative process is convergent (it is in fact rapidly convergent for broad layers) the solution requires only solving a few non-linear algebraic equations at each value x. As a constant x-spacing is not required in this process, the algebraic equation (29) for ϕ can be added to a predictor-corrector scheme for solving the coupled differential equations (10) for the

magnetic vector a. This is particularly interesting when mixed boundary layers (i.e., boundary layers with both electron and ion-gyroradii as characteristic scale lengths) are involved.

Although other methods for solving boundary value differential equations could in principle be applied to this problem, as for instance, the conjugate gradient algorithm [16] or the strongly implicit procedure of Stone [17], these methods usually boil down, at least conceptually, to the solution of large numbers of simultaneous non-linear equations solved by linearization and iteration. Another interesting approach could be the use of the simultaneous overrelaxation (SOR) method [18] for which an initial distribution $\phi(t, x)$ relaxes to an equilibrium with time derivative vanishing as $t \to \infty$. However, most of these alternative methods use a constant x-spacing. Therefore, for mixed transition layers, the simultaneous solution of Eqs. (9) and (10) by these methods should imply a sufficiently small (and constant) x-spacing to be able to describe the very thin electron layers embedded in a broader ion layer. The number of algebraic equations to be solved simultaneously would increase accordingly and the computer storage available to implement these methods should be large enough.

However, the method we have introduced in this paper provides an interesting and completely different numerical procedure which is conceptually simpler and is somewhat more physical. Furthermore, it does not require a large computer storage.

4. Solving Poisson's Equation in an Ion-Dominated Layer

In this section, we consider a TD separating a hot hydrogen plasma from a cooler one. The velocity distribution function for the electrons as a whole is isotropic since an ion-dominated layer is assumed. This layer has plasma boundary conditions characterized by eight plasma parameters as listed in Table I. Across the transition region, the temperature and density of each plasma species are respectively $\theta(x)$ and $n(x)$. Asymptotically, $\theta(\pm\infty) = T$, $n(-\infty) = N_\ell$ and $n(+\infty) = N_r$. The magnetic field at $x = -\infty$ is assumed to be 40 nT.

TABLE I

Plasma Boundary Conditions and Parameters of Velocity Distribution Functions for the Ion-Dominated Layer Illustrated in Fig. 1.

ν	Z	Species	T(eV)	N_ℓ(cm^{-3})	N_r(cm^{-3})	C_ℓ	C_r
1	−1	Electrons	2500	0.5	0	1	0
2	−1	Electrons	2500	0	0.15	0	1
3	+1	Protons	12.000	0.5	0	1	0
4	+1	Protons	3000	0	0.15	0	1

These plasma parameters correspond to two interpenetrated hydrogen plasmas with different characteristics. They correspond to typical magnetospheric plasma populations. The values of the parameters C_ℓ and C_s (see Eq. (3)) are also given in this table. From (3), it can be seen that they are consistent with the fact that the plasma from $x=-\infty$ (/from $x=+\infty$) is absent at $x=+\infty$ (/$x=-\infty$).

From Table I and from (5), the number densities (n) for each plasma species can be written

$$n^{(1)}=\frac{1}{2}\alpha^{(1)}\exp\left(\frac{e\phi}{kT^-}\right)\operatorname{erfc}\left(\frac{a}{2^{1/2}R_\ell^- B_\ell}\right) \tag{31}$$

$$n^{(2)}=\frac{1}{2}\alpha^{(2)}\exp\left(\frac{e\phi}{kT^-}\right)\operatorname{erfc}\left(-\frac{a}{2^{1/2}R_s^- B_s}\right) \tag{32}$$

$$n^{(3)}=\frac{1}{2}\alpha^{(3)}\exp\left(-\frac{e\phi}{kT^{(3)}}\right)\operatorname{erfc}\left(\frac{a}{2^{1/2}R_\ell^{(3)} B_\ell}\right) \tag{33}$$

$$n^{(4)}=\frac{1}{2}\alpha^{(4)}\exp\left(-\frac{e\phi}{kT^{(4)}}\right)\operatorname{erfc}\left(-\frac{a}{2^{1/2}R_s^{(4)} B_s}\right), \tag{34}$$

where $T^-=T^{(1)}=T^{(2)}$ ($=2500$ eV),

$$R_\ell^- B_\ell=R_s^- B_s=\left(\frac{m^- kT^-}{e^2}\right)^{1/2}.$$

Let us now choose the electric potential at $x=-\infty$ equal to zero, i.e.,

$$\phi(-\infty)=0; \tag{35}$$

then, the parameters α in Eqs. (31)–(34) can be seen to be related to the asymptotic densities and to the value of ϕ at $x=+\infty$. Taking the plasma neutrality at $x=\pm\infty$ into account, i.e.,

$$N_\ell^{(1)}=N_\ell^{(3)}=N_\ell\ (=0.5\ \text{cm}^{-3}) \tag{36}$$

$$N_s^{(2)}=N_s^{(4)}=N_s\ (=0.15\ \text{cm}^{-3}), \tag{37}$$

one obtains (assuming that $B(x)>0$, so that $a(-\infty)=-\infty$ and $a(+\infty)=+\infty$)

$$\alpha^{(1)}=\alpha^{(3)}=N_\ell \qquad (=0.5\ \text{cm}^{-3}) \tag{38}$$

$$\alpha^{(2)}\exp\left[\frac{e\phi(+\infty)}{kT^-}\right]=\alpha^{(4)}\exp\left[-\frac{e\phi(+\infty)}{kT^{(4)}}\right]$$

$$=N_s \qquad (=0.15\ \text{cm}^{-3}). \tag{39}$$

As the electron velocity distribution as a whole is isotropic, Eq. (3) implies that $\alpha^{(2)}$ must be identical to $\alpha^{(1)}$. Therefore, from (38) and (39)

$$\phi(+\infty) = \frac{kT^-}{e} \ln\left(\frac{N_s}{N_\ell}\right) (= -3009.932 \text{ V}) \tag{40}$$

$$\alpha^{(4)} = N_s \left(\frac{N_s}{N_\ell}\right)^{T^-/T^{(4)}} \quad (\approx 0.055 \text{ cm}^{-3}). \tag{41}$$

The electron density throughout the transition is then

$$n^-(x) = n^{(1)} + n^{(2)} = N_\ell \exp\left[\frac{e\phi(x)}{kT^-}\right]. \tag{42}$$

Of course, Eq. (42) represents a Maxwellian distribution of electrons in the field of a conservative force (the electric field) acting on them. Consequently, the electrons do not contribute to the current density. This can be seen directly from (6) since $j^{(1)} = -j^{(2)}$ and $j^- = 0$. Therefore, the current density inside the layer is only due to the protons and the characteristic thickness of this transition is the proton gyroradius [$R_\ell^{(3)} = 280$ km, $R_s^{(4)} = 86.5$ km with $B_z = 64.70$ nT].

Figure 1 illustrates the structure of the electric potential, electric field, and charge density for different orders of approximation in solving Poisson's equation. The distance across the transition is given in unit of the ion gyroradius at $x = -\infty$ (i.e., $R_\ell^+ = R_\ell^{(3)} = 280$ km). The bottom panels demonstrate that, on and after the first-order approximation, the electric potential is determined with a relative accuracy $|(\phi_3 - \phi_i)/\phi_3|$ $(i = 1, 2)$ much less than 10^{-7}. The quasi-neutrality approximation (ϕ_0) still remains a very good approximation, since $|(\phi_1 - \phi_0)/\phi_1|$ is less than 3×10^{-6}. It can also be seen that, on and after the first-order approximation, the

approximations. This means that the iterations are converging in cases of ion-dominated layers. Note also that the relative error on ϕ_0 considered as an approximate solution of Poisson's equation (i.e., 3×10^{-6}) is of the order of the relative charge density Q_0/en^- (n^- being the total electron density).

5. Solving Poisson's Equation in an Electron-Dominated Layer

The plasma parameters in the case of an electron-dominated layer are given in Table II. The magnetic field at $x = -\infty$ is 40 nT. In this example, $T^{(1)} = T^{(2)} = T^- = 2500$ eV and $T^{(3)} = T^{(4)} = T^+ = 5000$ eV.

The expressions for the number densities (n) are similar to the ones given by Eqs. (31)–(34) with $T^{(3)} = T^{(4)} = T^+$ and

$$R_\ell^{(3)} B_\ell = R_s^{(4)} B_s = \left(\frac{m^+ kT^+}{e^2}\right)^{1/2}.$$

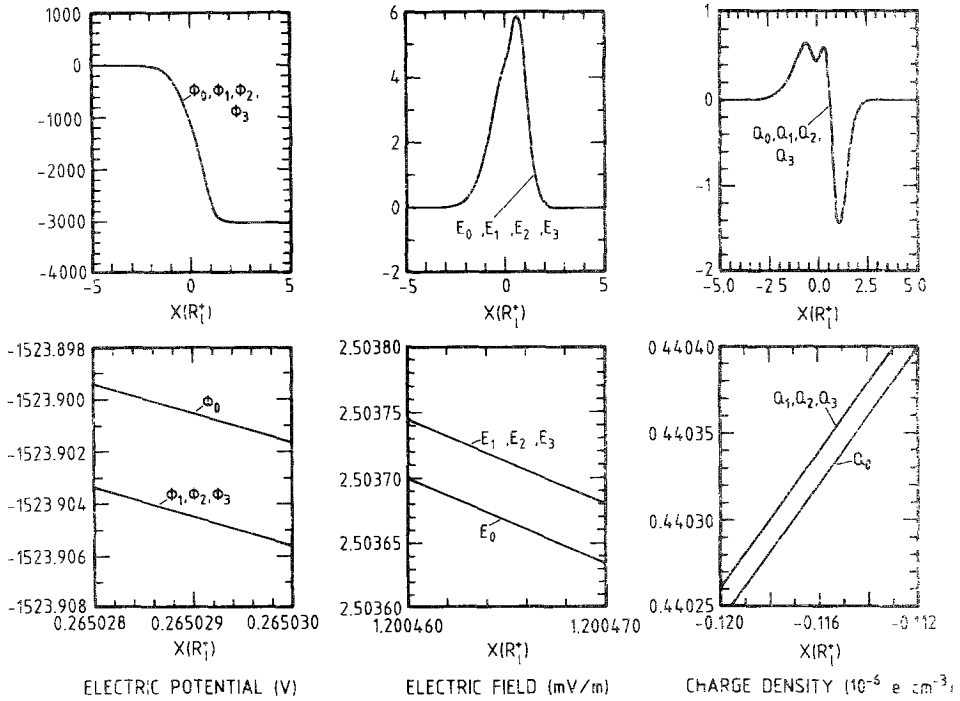

FIG. 1. Electric structure of an ion-dominated layer. Plasma boundary conditions are given in Table I. The magnetic field at $x = -\infty$ is 40 nT. The ion gyroradius ($R_i^+ = R_i^{(3)} = 280$ km) is the characteristic scale length. The left-hand side panels display the electric potential (ϕ), while the electric field (E) and the charge density (Q) are represented in the middle and right-hand side panels, respectively. Approximations of the solution of Poisson's equation are displayed up to the third order. The bottom panels are enlargements of a tiny small section of the layer. It can be seen that the successive approximations are very rapidly converging to a solution. This solution still remains very close to the result obtained from the quasi-neutrality approximation or zero-order approximation (within a precision of 3×10^{-6}). The relative error on ϕ_0 can be seen to be of the order of Q_0/en^- (n^- being the total electron density).

TABLE II

Plasma Boundary Conditions and Parameters of Velocity Distribution Functions for the Electron-Dominated Layer Illustrated in Fig. 2 and 3.

v	Z	Species	T(eV)	N_r(cm^{-3})	N_s(cm^{-3})	C_r	C_s
1	−1	Electrons	2500	0.5	0	1	0
2	−1	Electrons	2500	0	0.4	0	1
3	+1	Protons	5000	0.5	0	1	0
4	+1	Protons	5000	0	0.4	0	1

Assuming (35) to hold and $B(x)>0$, the plasma neutrality at $x=\pm\infty$ imposes

$$\alpha^{(1)}=\alpha^{(3)}=N_\ell \qquad (=0.5\ \mathrm{cm}^{-3}) \tag{43}$$

$$\alpha^{(2)}\exp\left[\frac{e\phi(+\infty)}{kT^-}\right]=\alpha^{(4)}\exp\left[-\frac{e\phi(+\infty)}{kT^+}\right]=N_s \qquad (=0.4\ \mathrm{cm}^{-3}). \tag{44}$$

As the ion velocity distribution as a whole is isotropic, (3) and (43) imply that

$$\alpha^{(4)}=\alpha^{(3)}=N_\ell \qquad (=0.5\ \mathrm{cm}^{-3}). \tag{45}$$

Therefore, from (44) and (45),

$$\phi(+\infty)=-\frac{kT^+}{e}\ln\left(\frac{N_s}{N_\ell}\right) \qquad (=1115.718\ \mathrm{V}) \tag{46}$$

$$\alpha^{(2)}=N_s\left(\frac{N_s}{N_\ell}\right)^{T^+/T^-} \qquad (=0.256\ \mathrm{cm}^{-3}). \tag{47}$$

The proton density throughout the transition is then

$$n^+(x)=n^{(3)}+n^{(4)}=N_\ell\exp\left[-\frac{e\phi(x)}{kT^+}\right]. \tag{48}$$

As expected, (48) represents a Maxwellian distribution of protons in the field of a conservative force (the electric field) acting on them. Consequently, the protons do not contribute to the current density.

Indeed, from (6), $j^{(3)}=-j^{(4)}$ and $j^+=0$. Therefore the current density inside the layer is only due to the electrons and the characteristic thickness is the electron gyroradius [$R_\ell^{(1)}=2.98$ km, $R_s^{(2)}=2.73$ km with $B_s=43.61$ nT].

Figure 2 illustrates the structure of the electric potential, electric field and charge density up to the fourth order in solving Poisson's equation by the iteration method explained in Section 3. The distance across the transition is given in units of the electron gyroradius at $x=-\infty$ (i.e., $R_\ell^-=R_\ell^{(1)}=2.98$ km). It can be seen that $|(\phi_4-\phi_0)/\phi_4|$ is of the order of 6×10^{-3}, while $|(\phi_4-\phi_1)/\phi_4|$ is of the order of 5×10^{-4}. It can also be seen that each successive approximation ϕ_i ($i=0,\ldots,3$) reduces the relative error on ϕ, $|(\phi_4-\phi_i)/\phi_4|$, by roughly a factor of 10. These successive approximations converge to an single solution, since the differences between them decrease as the order of approximation increases. This is illustrated in the lower panels: the successive charge densities Q_i ($i=0,\ldots,4$) converge to an asymptotic solution located between the Q_3- and Q_4-curves. As previously noted, the relative error on ϕ_0, considered as an approximate solution of Poisson's equation (i.e., 6×10^{-3}) is again of the order of Q_0/en^-.

The maximum error in the electric field intensity using the quasi-neutrality approximation can be seen to be less than 3%. This maximum error occurs at the center of the transition region, where the gradient of the potential is maximum.

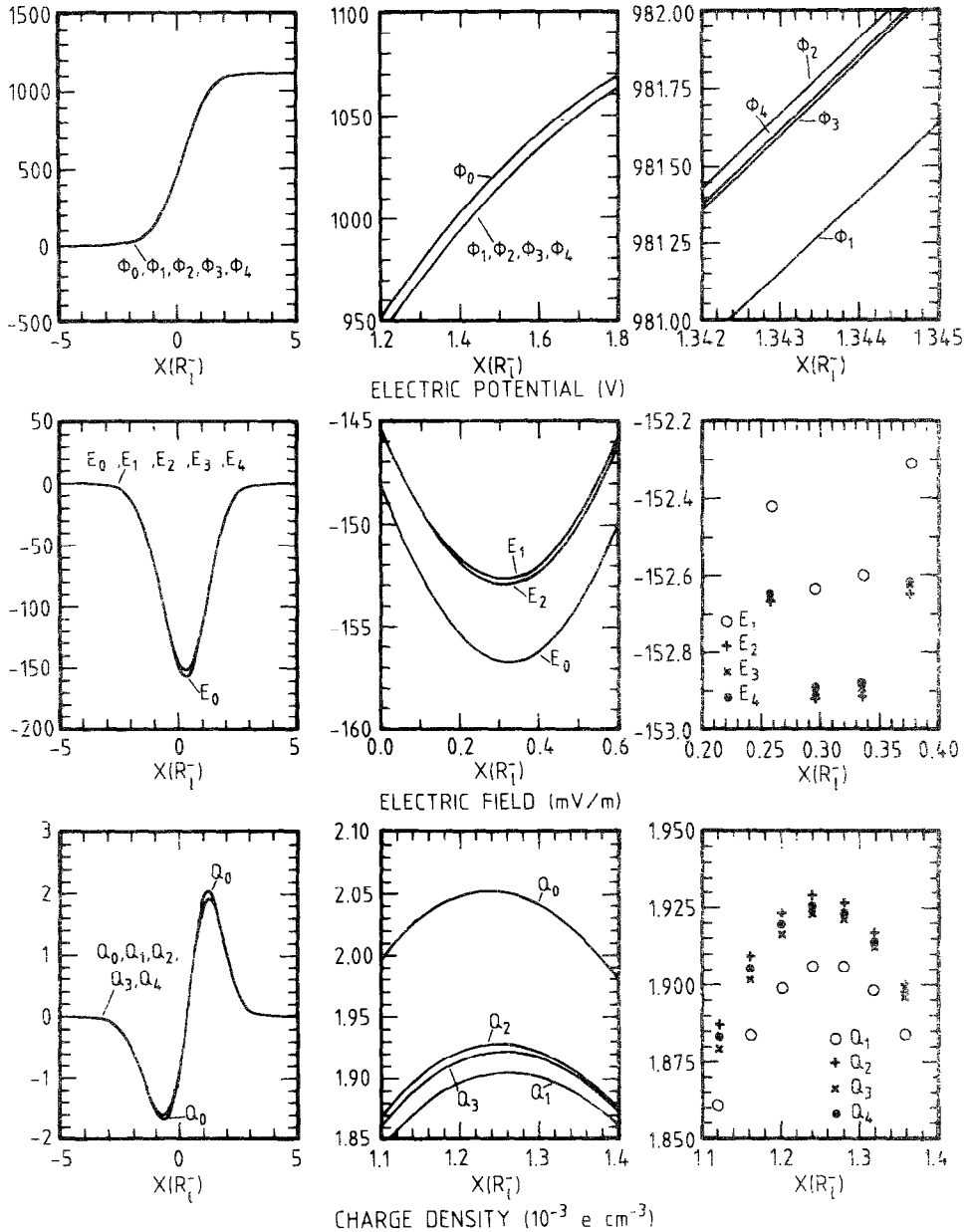

FIG. 2. Electric structure of an electron-dominated layer. Plasma boundary conditions are given in Table II. The magnetic field at $x = -\infty$ is 40 nT. The electron gyroradius ($R_i^- = R_i^{(1)} = 2.98$ km) is the characteristic scale length. The above panels display the electric potential (ϕ) while the electric field (E) and the charge density (Q) are represented in the middle and bottom panels, respectively. Approximations of the solution of Poisson's equation are displayed up to the fourth order. Panels in the second and third columns are enlargements of small or tiny sections of the layer. It can be seen that the successive approximations are converging to a solution. In this example, the characteristic thickness (D) is of the order of five Debye lengths (λ). Note that each successive approximation reduces the relative error on ϕ by roughly a factor of 10. The relative error on ϕ_0 is still of the order of Q_0/en^- (n^- being the total electron density). In this example, the solution ϕ_0 obtained from the quasi-neutrality approximation holds within a precision of 6×10^{-3}.

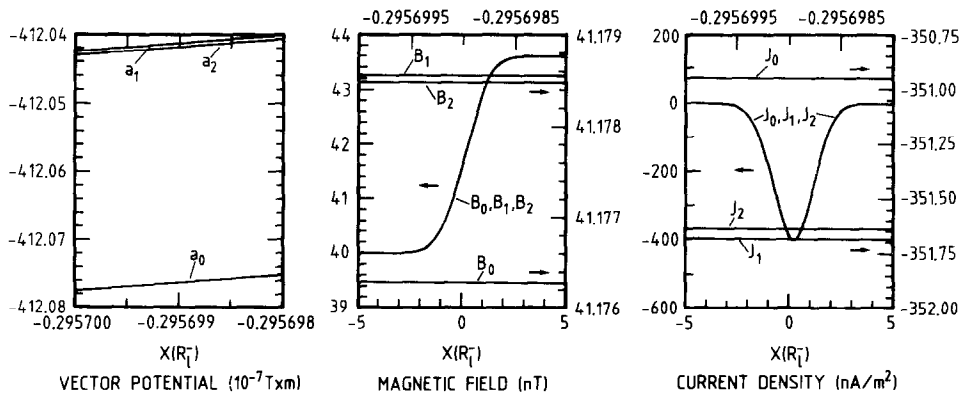

FIG. 3. An illustration showing that a, B, and J (the total current density, $J=\sum j$) are not very sensitive to the order of approximation in solving Poisson's equation. For the electron-dominated layer considered in this example (same as Fig. 2), this result is more specifically true on and after the first-order approximation. Because a, B, and J do not change significantly when the order of approximation becomes larger than 2, (29) can be decoupled from Eqs. (10) and (12) when considering approximations with order equal to (or larger than) 3.

Note also that the charge density in this electron-dominated layer is about 10^3 times larger than the corresponding charge density computed in the ion-dominated layer illustrated in Fig. 1. In Fig. 1 and 2, the Debye length (λ_ℓ) at $x=-\infty$ is 526 m. In the electron-dominated layer shown in Fig. 2, the Debye length at $x=+\infty$, (λ_ℓ) is 588 m while the characteristic thickness D lies between $R_\ell^- =$ 2.98 km and $R_i^- = 2.73$ km, i.e., $D/\lambda \approx 4.65 - 5.67$. For such thicknesses ($D \geqslant 5\lambda$), the method of successive approximations remains a convergent one and, furthermore, the quasi-neutrality approximation is still a reasonable approximation which can be used for all practical purposes.

In Fig. 1 and 2, E_2 and Q_2 have been calculated numerically by a Lagrangian method of interpolating polynomial. Third-order (Fig. 1 and 2) and fourth-order (Fig. 2) approximations have been successively determined as solutions of (29) while keeping the second-order approximation (a_2, B_2) for a and B. For the plasma boundary conditions given in Table II, Fig. 3 indicates that a and B are not very sensitive to the order of approximation in solving Poisson's equation. Indeed, it can be seen that a_2, B_2, and J_2 (the total current density) do not differ significantly from a_1, B_1, and J_1 (the differences are even much less in ion-dominated layers such as the one illustrated in Fig. 1). Therefore, on and after the third order, it is quite justified to decouple (29) from Eqs. (10) and (12) as done in this paper.

At this stage, it can be asked whether convergence is still achieved when the thickness D schrinks to a few Debye lengths λ. The results presented in Fig. 4 illustrate such a case of a sharper boundary layer. The plasma and magnetic field

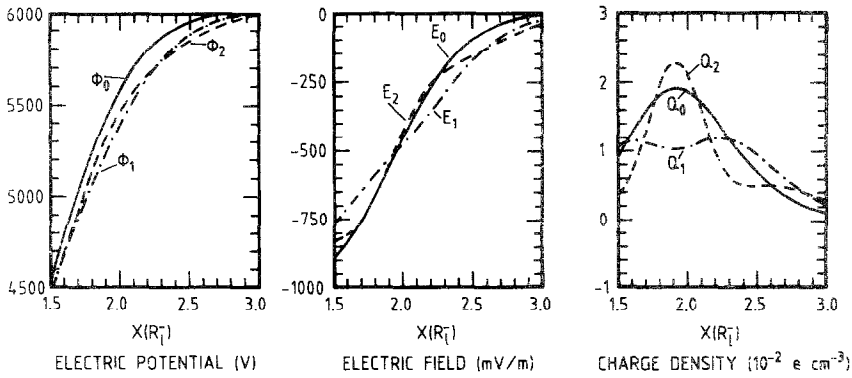

FIG. 4. Electric structure of an electron-dominated layer. The plasma and magnetic field boundary conditions are identical to those pertaining to Fig. 2, except that, at $x = +\infty$, the number density of the particles of either sign has been lowered ($N_\infty = 0.15\ \text{cm}^{-3}$). The electron gyroradius ($R_i^- = R_i^{(1)} = 2.98$ km) is the characteristic scale length. In this example, the Debye length on the right-hand side of the transition is 960 m, i.e., a small fraction of the electron gyroradius ($R_i^- = 2.31$ km). It can be seen that, for positive values of x ($x \sim 1.5 - 3R_i^-$), the successive approximations for Q_i do not converge to a solution, since higher order approximations differ more and more from lower ones. Note that the charge density in this example is 10 times larger than the one illustrated in Fig. 2.

that the transition is an electron-dominated layer ($\phi(+\infty) \simeq 6020$ V, $\alpha^{(2)} = 0.0135\ \text{cm}^{-3}$).

Because the number density at $x = +\infty$, (N_∞) has been reduced, the Debye length at the right-hand side of this transition increases ($\lambda_\infty = 960$ m). In this example, the Debye length (λ_∞) is a small fraction ($R_i^-/\lambda_\infty = 2.41$) of the electron gyroradius at $x = +\infty$ ($R_i^- = 2.31$ km) and it can be seen from Fig. 4, that for positive values of x($x \sim 1.5 - 3R_i^-$), the successive approximations do not converge to an asymptotic solution, since higher order approximations for Q_i differ more and more from lower ones. It can therefore be concluded that when D is of the order of $1 - 3\lambda$, the method of successive approximations for solving Poisson's equation breaks down. Note also that the charge density in this example is 10 times larger than the one illustrated in Fig. 2.

It can also be concluded that in the case where the plasma density approaches zero on one side (i.e., plasma-free magnetic field on one side of the TD and field-free plasma on the other) the iterative method proposed above will fail to converge, since when the plasma density approaches zero the Debye length grows indefinitely and the quasi-neutrality approximation always fails to be valid at the outermost edge of the plasma region. This is the case of the classical Ferraro [19] cold plasma sheath model: an early attempt to describe the solar wind-magnetosphere interaction region as a TD between a vacuum geomagnetic field on one side and a cold streaming solar wind on the other. The basic feature of this model was that the random thermal speed of the solar wind was assumed to be small compared to the organized streaming velocity.

An attempt to improve the quasi-neutrality approximation in the case of the cold plasma sheath model was made by Sestero [20]. For that model, which shows large charge separation effects, Sestero found that Poisson's equation could be solved by a Runge–Kutta integration scheme. This result seems to indicate that Runge–Kutta or Hamin integration methods could be used when the thickness of the transition becomes smaller than a few Debye lengths, i.e., when charge separation effects cease to be negligible. It can therefore be expected that when the method of successive approximations fails to converge, i.e., when the electric charge density becomes large, usual integration methods such as Runge–Kutta or Hamin predictor-corrector scheme could successfully be used instead.

6. Conclusions

From this study of Poisson's equation in collisionless TD, it can be concluded that the difficulty in solving this second-order differential equation by standard computational methods, such as Runge–Kutta or Hamin schemes, can be avoided in many practical problems by using the so-called quasi-neutrality approximation. For the broad ion-dominated layer illustrated in Fig. 1 ($D \sim 10^2 - 10^3\lambda$), the relative error of the quasi-neutral solution is of the order of 10^{-5}–10^{-6} for the electric potential.

For the thin electron-dominated layer illustrated in Fig. 2 ($D \approx 5\lambda$), the quasi-neutrality approximation holds to a relative precision of the order of 10^{-2}–10^{-3}. In this electron-dominated layer, the error on ϕ can be reduced by considering higher order approximations. Each successive approximation reduces the relative error on ϕ roughly by a factor of 10. However, as illustrated in Fig. 4, when the characteristic thickness of an electron-dominated layer shrinks to a value less than 3λ, the method of successive approximations for solving Poisson's equation fails. In these sharp transition layers, the relative charge density is generally larger than 10^{-2}. In that case, it is expected that Runge–Kutta or Hamin schemes could be stable integration methods.

In all cases illustrated in this paper, the relative error on ϕ_0 is of the order of Q_0/en^- (the relative charge density). This means that, even in very sharp transitions with $D \approx 3\lambda$, the potential obtained by solving the quasi-neutrality approximation does not differ from the true solution by more than a few percent.

Since, in space plasmas, the Debye length is generally much smaller than the characteristic scale lengths of density and field variations, the quasi-neutrality approximation can be used with much confidence in all cases, even in sharp transitions like those involved in the mechanism of generation of discrete auroral arcs as proposed by Evans *et al.* [21] and Roth *et al.* [22]. Although the charge-neutrality approximations were used in these studies, the conclusions that were deduced therein remain unaltered, in light of the present study.

The iterative method of successive approximations, that has been developed in this paper to solve Poisson's equation in the case of TDs, is suitable when an

improvement in the electric potential accuracy is desirable, particularly when the thickness of the transition region shrinks to $D \sim 5\lambda$. But, even in this case, the correction on the quasi-neutral solution does not exceed 1%.

It has also been shown that the modifications of the electrostatics resulting from the consideration of higher order approximations leave the magnetic field distribution virtually unchanged (see Fig. 3). Therefore, early in the process of iteration, Poisson's equation can be decoupled from the equation governing the magnetic field. In particular, when the magnetic field coupling is weak, manipulation of the turgid ϕ_1'' function in the Appendix can probably be avoided by already ignoring the magnetic field coupling from the second order approximation. In that case, computation of ϕ_1'' can be made directly by a Lagrangian method of interpolating polynomial.

When applied to purely electrostatic problems involving solely a non-linear Poisson's equation with source of charge depending on the electrostatic potential, the application of the iteration process is then straightforward. Indeed, as a consequence of the absence of magnetic field coupling, the Laplacian of each ϕ_n can then be computed directly by the usual Lagrangian method without resorting to explicit expressions for the second derivatives of lower order solutions.

Generally speaking, the iterative method of successive approximations developed in this paper can be easily extended to any problems involving a non-linear Poisson's equation with a right-hand side member depending on the actual potential solution. Compared to other numerical methods, this one is conceptually simpler, has a more physical ground, does not require a constant x-spacing and need no large computer storage.

Appendix

The first-order approximation ϕ_1 is solution of (28), i.e.,

$$\sum Zn(a_1, \phi_1) = -\frac{\varepsilon_0}{e}\phi_0''(a_1, \phi_1, B_1). \tag{28}$$

where ϕ_0'' is given by (22).

By deriving (28) once and twice with respect to x, one obtains expressions for $\phi_1'(a_1, \phi_1, B_1)$ and $\phi_1''(a_1, \phi_1, B_1)$, respectively (note that the derivative rules for j_{rst} are similar to those given for J_{rst}: use j instead of J in (25) and (26)). It is found that

$$\phi_1' = -\frac{J_{010} + (\varepsilon_0/e)[\mu_0 N_{100}^{-1}(j_{000} Y + a_1 j_{001} J_{010}) + B_1^2 G]}{(N_{100} + (\varepsilon_0/e) W)} B_1 \tag{A.1}$$

with

$$Y = 3a_1 J_{011} - 5N_{100}^{-1} J_{110} J_{010} + 2N_{100}^{-2} J_{010}^2 N_{200} \tag{A.2}$$

$$G = -N_{100}^{-1}(J_{011} + a_1^2 J_{012}) + a_1 N_{100}^{-2}(3J_{110} J_{011} + 2J_{010} J_{111}) - N_{100}^{-3} J_{010}(4J_{110}^2 + 2a_1 J_{011} N_{200} + J_{010} J_{210}) + 3N_{100}^{-4} J_{010}^2 J_{110} N_{200} \tag{A.3}$$

$$W = \mu_0 N_{100}^{-1}(j_{000} J_{110} - j_{000} N_{100}^{-1} N_{200} J_{010} + j_{100} J_{010}) - a_1 B_1^2 N_{100}^{-1} J_{111} + B_1^2 N_{100}^{-2}(2J_{110}^2 + 2J_{010} J_{210} + a_1 J_{011} N_{200}) - B_1^2 N_{100}^{3} J_{010}(J_{010} N_{300} + 6J_{110} N_{200}) + 3B_1^2 N_{100}^{4} N_{200}^2 J_{010}^2 \tag{A.4}$$

and

$$\phi_1'' = \frac{1}{(N_{100} + (\varepsilon_0/e) W)} \times \left[-\frac{\varepsilon_0}{e} S - \phi_1'^2 N_{200} - 2B_1^2 \phi_1' J_{110} + \mu_0 j_{000} J_{010} - a_1 B_1^2 J_{011} \right] \tag{A.5}$$

with

$$S = \alpha_1 \phi_1'^2 + \alpha_2 B_1^2 + \alpha_3 (\mu_0 j_{000})^2 + 2\alpha_4 B_1 \phi_1' - 2\alpha_5 \mu_0 j_{000} \phi_1' - 2\alpha_6 \mu_0 j_{000} B_1 - \beta_1 \mu_0 j_{000} - \beta_2 \mu_0 (j_{100} \phi_1' + j_{001} a_1 B_1), \tag{A.6}$$

where

$$\alpha_1 = \mu_0 j_{000} N_{100}^{-1}(-2N_{100}^{-1} N_{200} J_{110} + J_{210} + 2N_{100}^{-2} N_{200}^2 J_{010} - N_{100}^{-1} N_{300} J_{010}) + 2\mu_0 j_{100} N_{100}^{-1}(J_{110} - N_{100}^{-1} N_{200} J_{010}) + \mu_0 j_{001} N_{100}^{-1} J_{011} + B_1^2 N_{100}^{-2}(2a_1 N_{200} J_{011} - a_1 N_{300} J_{010}) - 10N_{100}^{-1} N_{200} J_{110}^2 + 6J_{110} J_{210} - 10N_{100}^{-1} N_{200} J_{010} J_{210} + 2J_{010} J_{310} - 2a_1 N_{100}^{-1} N_{200}^2 J_{011} + a_1 J_{011} N_{300} + 9N_{100}^{-2} N_{200} J_{010}^2 N_{300} - 8N_{100}^{-1} J_{010} J_{110} N_{300} - N_{100}^{-1} J_{010}^2 N_{400} + 24N_{100}^{-2} N_{200}^2 \times J_{010} J_{110} - 12N_{100}^{-3} N_{200}^3 J_{010}^2) \tag{A.7}$$

$$\alpha_2 = \mu_0 N_{100}^{-1}(j_{000} J_{011} - 2a_1 N_{100}^{-1} J_{110} j_{000} J_{011} + 2a_1^2 j_{001} J_{011} + a_1^2 j_{000} J_{012} + 2N_{100}^{-2} J_{110}^2 j_{000} J_{010} - 2a_1 N_{100}^{-1} j_{001} J_{110} J_{010} - a_1 N_{100}^{-1} j_{000} J_{111} J_{010} + j_{001} J_{010} + a_1^2 j_{002} J_{010}) - a_1 B_1^2 N_{100}^{-1}(3J_{012} + a_1^2 J_{013}) + B_1^2 N_{100}^{-2}(4a_1^2 J_{110} J_{012} + 4J_{110} J_{011} + 5a_1^2 J_{111} J_{011}$$

$$+ 2J_{010}J_{111} + 2a_1^2 J_{010}J_{112}) - B_1^2 N_{100}^{-3}(10a_1 J_{110}^2 J_{011}$$
$$+ 12a_1 J_{110}J_{010}J_{111} + 2J_{010}J_{011}N_{200}$$
$$+ 2a_1^2 J_{011}^2 N_{200} + 2a_1^2 J_{010}J_{012}N_{200} + 4a_1 J_{010}J_{011}J_{210}$$
$$+ a_1 J_{010}^2 J_{211}) + B_1^2 N_{100}^{-4}(12J_{110}^3 J_{010} + 12a_1 J_{110}J_{010}J_{011}N_{200}$$
$$+ 6J_{110}J_{010}^2 J_{210} + 3a_1 J_{010}^2 J_{111}N_{200}) - 12B_1^2 N_{100}^{-5} J_{110}^2 J_{010}^2 N_{200} \quad \text{(A.8)}$$

$$\alpha_3 = -2a_1 N_{100}^{-1} J_{011} + 4N_{100}^{-2} J_{010}J_{110} - 2N_{100}^{-3} J_{010}^2 N_{200} \quad \text{(A.9)}$$

$$\alpha_4 = \mu_0 N_{100}^{-1}(-a_1 N_{100}^{-1} N_{200} j_{000} J_{011} + a_1 j_{100} J_{011}$$
$$+ a_1 j_{000} J_{111} + 2N_{100}^{-2} N_{200} j_{000} J_{110} J_{010}$$
$$- N_{100}^{-1} j_{100} J_{110} J_{010} - N_{100}^{-1} j_{000} J_{210} J_{010} - N_{100}^{-1} j_{000} J_{110}^2$$
$$- a_1 N_{100}^{-1} N_{200} j_{001} J_{010} + a_1 j_{101} J_{010} + a_1 j_{001} J_{110})$$
$$- B_1^2 N_{100}^{-1}(J_{111} + a_1^2 J_{112}) + B_1^2 N_{100}^{-2}(N_{200}J_{011} + a_1^2 N_{200}J_{012}$$
$$+ 3a_1 J_{210}J_{011} + 5a_1 J_{110}J_{111} + 2a_1 J_{010}J_{211})$$
$$- B_1^2 N_{100}^{-3}(8a_1 N_{200}J_{110}J_{011} + 6a_1 N_{200}J_{010}J_{111} + 4J_{110}^3$$
$$+ 10J_{010}J_{110}J_{210} + 2a_1 J_{010}J_{011}N_{300} + J_{010}^2 J_{310})$$
$$+ B_1^2 N_{100}^{-4}(18N_{200}J_{010}J_{110}^2 + 6a_1 N_{200}^2 J_{010}J_{011} + 6N_{200}J_{010}^2 J_{210}$$
$$+ 3J_{010}^2 J_{110}N_{300}) - 12B_1^2 N_{100}^{-5} N_{200}^2 J_{010}^2 J_{110} \quad \text{(A.10)}$$

$$\alpha_5 = 2B_1 N_{100}^{-2}(a_1 N_{200}J_{011} - a_1 N_{100}J_{111}$$
$$- 6N_{100}^{-1} N_{200}J_{010}J_{110} + 2J_{110}^2 + 2J_{010}J_{210}$$
$$+ 3N_{100}^{-2} N_{200}^2 J_{010}^2 - N_{100}^{-1} J_{010}^2 N_{300}) \quad \text{(A.11)}$$

$$\alpha_6 = -2B_1 N_{100}^{-1}(J_{011} + a_1^2 J_{012})$$
$$+ a_1 B_1 N_{100}^{-2}(6J_{110}J_{011} + 4J_{010}J_{111})$$
$$- B_1 N_{100}^{-3}(8J_{010}J_{110}^2 + 4a_1 J_{010}J_{011}N_{200} + 2J_{010}^2 J_{210})$$
$$+ 6B_1 N_{100}^{-4} J_{010}^2 J_{110} N_{200} \quad \text{(A.12)}$$

$$\beta_1 = \mu_0 a_1 N_{100}^{-1} j_{000} J_{011} - \mu_0 N_{100}^{-2} j_{000} J_{110} J_{010}$$
$$+ \mu_0 a_1 N_{100}^{-1} j_{001} J_{010} - B_1^2 N_{100}^{-1} J_{011} - a_1^2 B_1^2 N_{100}^{-1} J_{012}$$
$$+ 3a_1 B_1^2 N_{100}^{-2} J_{110}J_{011} + 2a_1 B_1^2 N_{100}^{-2} J_{010}J_{111}$$
$$- 4B_1^2 N_{100}^{-3} J_{010}J_{110}^2 - 2a_1 B_1^2 N_{100}^{-3} J_{010}J_{011}N_{200}$$
$$- B_1^2 N_{100}^{-3} J_{010}^2 J_{210} + 3B_1^2 N_{100}^{-4} J_{010}^2 J_{110} N_{200} \quad \text{(A.13)}$$

$$\beta_2 = -2a_1 B_1 N_{100}^{-1} J_{011} + 4B_1 N_{100}^{-2} J_{010}J_{110} - 2B_1 N_{100}^{-3} J_{010}^2 N_{200}. \quad \text{(A.14)}$$

ACKNOWLEDGMENTS

The authors acknowledge fruitful discussions with Dr. R. Barakat. They also thank the reviewers for their helpful comments.

REFERENCES

1. D. M. WILLIS, *J. Atmos. Terr. Phys.* **40**, 301 (1978).
2. V. FORMISANO, *Geophys. Res. Lett.* **9**, 1033 (1982).
3. A. NISHIDA, *Geomagnetic Diagnosis of the Magnetosphere* (Springer-Verlag, New York, 1978), p. 13.
4. L. F. BURLAGA AND N. F. NESS, *Solar Phys.* **9**, 467 (1969).
5. I. PAPAMASTORAKIS, G. PASCHMANN, N. SCKOPKE, S. J. BAME, AND J. BERCHEM, *J. Geophys. Res.* **89**, 127 (1984).
6. M. ROTH, in *Proceedings, XIX ESLAB Symposium on the Sun and the Heliosphere in Three Dimensions, Les Diablerets, Switzerland, 1985*, edited by R. G. Marsden (Astrophysics and Space Science Library, Reidel, Dordrecht, 1986), p. 167.
7. A. SESTERO, *Phys. Fluids* **7**, 44 (1964).
8. E. G. HARRIS, *Nuovo Cimento* **23**, 115 (1962).
9. J. LEMAIRE AND L. F. BURLAGA, *Astrophys. Space Sci.* **45**, 303 (1976).
10. M. ROTH, *J. Atmos. Terr. Phys.* **40**, 323 (1978).
11. M. ROTH, in *Proceedings, Magnetospheric Boundary Layers Conference, Alpbach, Austria, 1979*, edited by B. Battrick and J. Mort (ESTEC, Noordwijk, 1979), ESA SP-148, p. 295.
12. L. C. LEE AND J. R. KAN, *J. Geophys. Res.* **84**, 6417 (1979).
13. A. SESTERO, *Phys. Fluids* **9**, 2006 (1966).
14. E. C. WHIPPLE, J. R. HILL, AND J. D. NICHOLS, *J. Geophys. Res.* **89**, 1508 (1984).
15. R. P. BRENT, *Algorithms for Minimization without Derivatives* (Prentice-Hall, Englewood Cliffs, NJ, 1973), Chaps. 3, 4.
16. H. A. VAN DER VORST, *J. Comput. Phys.* **44**, 1 (1981).
17. H. J. STONE, *SIAM J. Num. Anal.* **5**, 530 (1968).
18. J. STOER AND R. BULIRSCH, *Introduction to Numerical Analysis* (Springer-Verlag, New York, 1980). Sections 8.3–8.5.
19. V. C. A. FERRARO, *J. Geophys. Res.* **57**, 15 (1952).
20. A. SESTERO, *Phys. Fluids* **8**, 739 (1965).
21. D. S. EVANS, M. ROTH, AND J. LEMAIRE, in *Proceedings, NASA Workshop on Double Layers in Astrophysics, Huntsville, 1986*, edited by A. C. Williams and T. W. Moorehead (NASA Conference Publication 2469, Marshall Space Flight Center, Alabama, 1987), p. 287.
22. M. ROTH, D. S. EVANS, AND J. LEMAIRE, in *Proceedings, Electromagnetic Wave Propagation Panel Spring 1986 Symposium on the Aerospace Environment at High Altitudes and Its Implications for Spacecraft Charging and Communications, The Hague, The Netherlands, 1986*, edited by NATO (AGARD Conference Proceedings CP – 406, AGARD-NATO, Neuilly-sur-Seine, France, 1987), p. I-22.